DISCRETIZATION OF PARAMETRIC ANALOG CIRCUITS FOR REAL-TIME SIMULATIONS

Kristjan Dempwolf, Martin Holters and Udo Zölzer

Dept. of Signal Processing and Communications,
Helmut Schmidt University Hamburg
Hamburg, Germany
kristjan.dempwolf|martin.holters|udo.zoelzer@hsuhh.de

ABSTRACT

The real-time simulation of analog circuits by digital systems becomes problematic when parametric components like potentiometers are involved. In this case the coefficients defining the digital system will change and have to be adapted. One common solution is to recalculate the coefficients in real-time, a possibly computationally expensive operation.

With a view to the simulation using state-space representations, two parametric subcircuits found in typical guitar amplifiers are analyzed, namely the tone stack, a linear passive network used as simple equalizer and a distorting preamplifier, limiting the signal amplitude with LEDs. Solutions using trapezoidal rule discretization are presented and discussed. It is shown, that the computational costs in case of recalculation of the coefficients are reduced compared to the related DK-method, due to minimized matrix formulations. The simulation results are compared to reference data and show good match.

1. INTRODUCTION

For the simulation of non-linear audio systems, e.g. guitar amplifiers or effect units, several methods are common. Most of them are based on the electrical relations of the original circuit, namely the use of wave digital filters [1] or state-space systems [2].

Typically the circuit of the reference system is split up into cascaded blocks whose input-output relation can be described by analytic expressions, non-linear equations or lookup tables. In this way it is possible to implement simulations that allow real-time computation. An introduction to the state of the art gives [3].

One big problem arises when component values are changed. In this case the arranged system has to be adapted. Common solutions are to calculate the coefficients for all relevant parameter values offline and store them in large lookup tables, or to perform a recomputation of the coefficients in real-time. In other words: the simulation of systems containing parametric components like potentiometers or variable capacitors comes along with either high computational costs or high memory requirements.

In this paper we discuss state-space models for two parametric audio circuits and present an alternative approach reducing the computational costs for recomputations.

2. STATE-SPACE REPRESENTATION OF LINEAR SYSTEMS

The state-space representation is a common tool in control engineering and system theory to describe physical systems. By defining suitable internal *states*, a system can be modeled as a set of input, output and state variables that are related by first-order differential equations.

2.1. Continuous-Time model

For a general linear system defined in continuous time we have

$$\dot{\boldsymbol{x}}(t) = \boldsymbol{A} \cdot \boldsymbol{x}(t) + \boldsymbol{B} \cdot \boldsymbol{u}(t) \tag{1}$$

$$\boldsymbol{y}(t) = \boldsymbol{D} \cdot \boldsymbol{x}(t) + \boldsymbol{E} \cdot \boldsymbol{u}(t) \tag{2}$$

with state variables $\boldsymbol{x}(t)$ and $\dot{\boldsymbol{x}}(t)$, inputs $\boldsymbol{u}(t)$ and outputs $\boldsymbol{y}(t)$. $\boldsymbol{A}$ is called the state-, $\boldsymbol{B}$ the input-, $\boldsymbol{D}$ the output- and $\boldsymbol{E}$ the feedthrough-matrix. In most cases the considered system will have single input and single output. The input-, output- and feedthrough-matrices are then reduced to column vector $\boldsymbol{b}$, row vector $\boldsymbol{d}$ and scalar e. Note that in the following, we will drop the time-dependence from the continuous-time variables for notational brevity.

For electric circuits the number of state variables needed is approximately given by the number of energy storage elements, e.g. a two-port network with 1 capacitor and 1 inductor requires 2 state variables. The analysis is based on network theory basics (Kirchhoff's circuit laws).

2.2. Discretization

The differential equation (1) describes a circuit, where $\boldsymbol{x}$ are the states, typically the voltages across capacitors, u is the input voltage and y is the output voltage. To obtain a discrete-time system from this continuous-time description, we apply the trapezoidal rule

$$\tfrac{T}{2}\big(\dot{\boldsymbol{x}}(n) + \dot{\boldsymbol{x}}(n-1)\big) = \boldsymbol{x}(n) - \boldsymbol{x}(n-1), \tag{3}$$

where T denotes the sampling interval. By substituting equation (1) in equation (3), this gives

$$\begin{aligned}\tfrac{T}{2}\big(\boldsymbol{A}\boldsymbol{x}(n) + \boldsymbol{b}u(n) + \boldsymbol{A}\boldsymbol{x}(n-1) + \boldsymbol{b}u(n-1)\big)& \\ = \boldsymbol{x}(n) - \boldsymbol{x}(n-1)&\end{aligned} \tag{4}$$

which can be solved for $\boldsymbol{x}(n)$ to obtain the state update equation

$$\begin{aligned}\boldsymbol{x}(n) = &\left(\tfrac{2}{T}\boldsymbol{I} - \boldsymbol{A}\right)^{-1} \\ &\cdot \big(\boldsymbol{b}u(n) + (\tfrac{2}{T}\boldsymbol{I} + \boldsymbol{A})\boldsymbol{x}(n-1) + \boldsymbol{b}u(n-1)\big).\end{aligned} \tag{5}$$

2.3. Canonicalization

Note that equation (5) requires not only the previous values of the states $\boldsymbol{x}(n-1)$, but also of the input $u(n-1)$ in addition to the current input value $u(n)$. We define the new state variable

$$\boldsymbol{x}_c(n) = \tfrac{T}{2}\big(\big(\tfrac{2}{T}\boldsymbol{I} + \boldsymbol{A}\big)\,\boldsymbol{x}(n) + \boldsymbol{b}u(n)\big) \tag{6}$$

and convert to a canonical representation by substituting

$$\boldsymbol{x}(n) = \big(\tfrac{2}{T}\boldsymbol{I} + \boldsymbol{A}\big)^{-1}\big(\tfrac{2}{T}\boldsymbol{x}_c(n) - \boldsymbol{b}u(n)\big), \tag{7}$$

which leads to

$$\begin{aligned}\big(\tfrac{2}{T}\boldsymbol{I} + \boldsymbol{A}\big)^{-1}&\big(\tfrac{2}{T}\boldsymbol{x}_c(n) - \boldsymbol{b}u(n)\big)\\ &= \big(\tfrac{2}{T}\boldsymbol{I} - \boldsymbol{A}\big)^{-1}\big(\boldsymbol{b}u(n) + \tfrac{2}{T}\boldsymbol{x}_c(n-1)\big)\end{aligned} \tag{8}$$

where no references to $u(n-1)$ occur anymore. To obtain the state update equation, we first left-multiply with $\big(\frac{2}{T}\boldsymbol{I} + \boldsymbol{A}\big)$, giving

$$\begin{aligned}\tfrac{2}{T}\boldsymbol{x}_c(n) - \boldsymbol{b}u(n) = \big(\tfrac{2}{T}\boldsymbol{I} + \boldsymbol{A}\big)&\big(\tfrac{2}{T}\boldsymbol{I} - \boldsymbol{A}\big)^{-1}\\ &\cdot\big(\boldsymbol{b}u(n) + \tfrac{2}{T}\boldsymbol{x}_c(n-1)\big)\end{aligned} \tag{9}$$

and then solve to

$$\begin{aligned}\boldsymbol{x}_c(n) = 2\big(\tfrac{2}{T}\boldsymbol{I} - \boldsymbol{A}\big)^{-1}&\boldsymbol{b}u(n)\\ &+ \big(\tfrac{2}{T}\boldsymbol{I} + \boldsymbol{A}\big)\cdot\big(\tfrac{2}{T}\boldsymbol{I} - \boldsymbol{A}\big)^{-1}\boldsymbol{x}_c(n-1)\end{aligned} \tag{10}$$

by using the relation

$$\big(\tfrac{2}{T}\boldsymbol{I} + \boldsymbol{A}\big)\big(\tfrac{2}{T}\boldsymbol{I} - \boldsymbol{A}\big)^{-1}\boldsymbol{b} + \boldsymbol{b} = \tfrac{4}{T}\big(\tfrac{2}{T}\boldsymbol{I} - \boldsymbol{A}\big)^{-1}\boldsymbol{b}. \tag{11}$$

The output equation then becomes

$$\begin{aligned}y(n) = \tfrac{2}{T}\boldsymbol{d}\big(\tfrac{2}{T}\boldsymbol{I} + \boldsymbol{A}\big)^{-1}&\boldsymbol{x}_c(n)\\ &+ \big(e - \boldsymbol{d}\big(\tfrac{2}{T}\boldsymbol{I} + \boldsymbol{A}\big)^{-1}\boldsymbol{b}\big)u(n)\end{aligned} \tag{12}$$

or, by substituting equation (10),

$$\begin{aligned}y(n) = \tfrac{2}{T}\boldsymbol{d}\big(\tfrac{2}{T}\boldsymbol{I} - \boldsymbol{A}\big)^{-1}&\boldsymbol{x}_c(n-1)\\ &+ \big(e + \boldsymbol{d}\big(\tfrac{2}{T}\boldsymbol{I} - \boldsymbol{A}\big)^{-1}\boldsymbol{b}\big)u(n).\end{aligned} \tag{13}$$

The latter form is advantageous because only the inverse matrix $\big(\frac{2}{T}\boldsymbol{I} - \boldsymbol{A}\big)^{-1}$ has to be computed for both state update and output equation. The final discrete-time system can then be written as

$$\boldsymbol{x}_c(n) = \bar{\boldsymbol{A}}\boldsymbol{x}_c(n-1) + \bar{\boldsymbol{b}}u(n) \tag{14}$$

$$\boldsymbol{y}(n) = \bar{\boldsymbol{d}}\boldsymbol{x}_c(n-1) + \bar{e}u(n) \tag{15}$$

with

$$\bar{\boldsymbol{A}} = \big(\tfrac{2}{T}\boldsymbol{I} + \boldsymbol{A}\big)\big(\tfrac{2}{T}\boldsymbol{I} - \boldsymbol{A}\big)^{-1} \tag{16}$$

$$\bar{\boldsymbol{b}} = 2\big(\tfrac{2}{T}\boldsymbol{I} - \boldsymbol{A}\big)^{-1}\boldsymbol{b} \tag{17}$$

$$\bar{\boldsymbol{d}} = \tfrac{2}{T}\boldsymbol{d}\big(\tfrac{2}{T}\boldsymbol{I} - \boldsymbol{A}\big)^{-1} \tag{18}$$

$$\bar{e} = e + \boldsymbol{d}\big(\tfrac{2}{T}\boldsymbol{I} - \boldsymbol{A}\big)^{-1}\boldsymbol{b}. \tag{19}$$

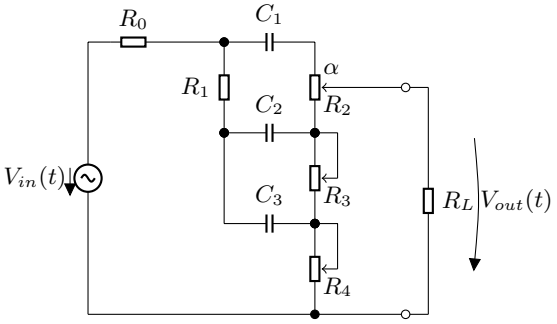

Figure 1: *Schematic of the Fender tone stack, type AA763.*

2.4. Schedule for linear Systems

The schedule for building a real-time linear system is:

1. State-space analysis of the circuit: Find a (symbolic) matrix formulation in the continuous-time domain. The voltages across the capacitors are defining states.
2. Perform a discretization (e.g. trapezoidal rule) to achieve the corresponding discrete-time representation.
3. Filtering process:
   - Compute the output samples for the given input.
   - Update the matrix entries in case of parameter modifications.

2.5. DK-method

The presented approach and its upcoming non-linear extension (section §4) is similar to the DK-method [2], but with some differences concerning the discretization step and the system description. The DK-method makes use of discrete-time state-space models and network formulations in accordance with the *Modified Nodal Analysis*, MNA. All energy storage elements have to be discretized component-wise before network analysis (e.g. trapezoidal rule integration), capacities and inductors therefore have to be replaced by companion circuits. The computation is in general similar to SPICE. A big advantage of the DK-method is the good applicability for automatization. Drawback: The MNA is a special form of the node voltage analysis and requires one expression in terms of Kirchhoff's current law for each node of the circuit. Thus even small electric circuits may result in huge, even though sparse, matrix representations.

3. APPLICATION: FENDER TONE STACK

A good example for a highly parametric linear system is given by the so-called *tone stack*, see Figure 1, which was already the subject in various previous works, e.g. [4]. This (or a similar) passive filter network can be found in most guitar amplifiers where it is used as a simple equalizer. Commonly the tone stack is placed between preamp and phase splitter. By adjusting the controls for bass (R_3), mid (R_4) and treble (R_2) the sound can be varied in a wide range. The frequency responses for different parameters are plotted exemplary in Figure 2. Note that the frequency bands

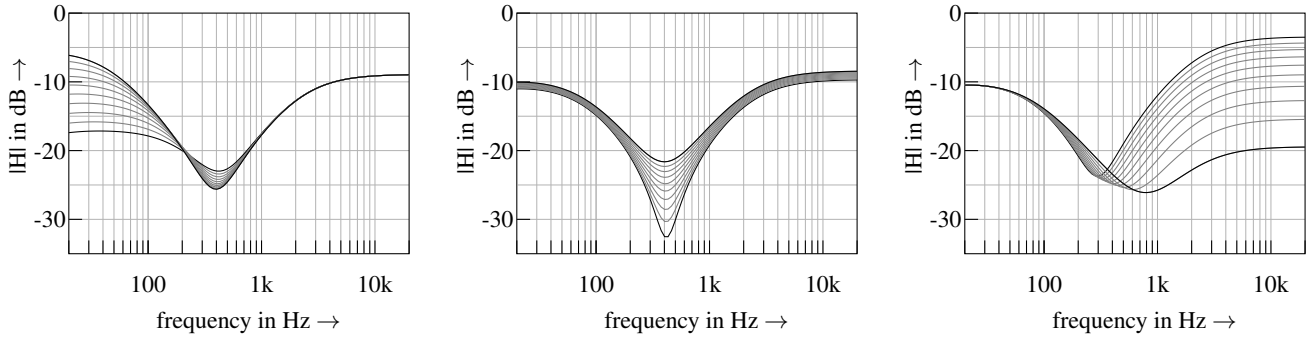

Figure 2: *Frequency response of the tone stack for different parameter sets. From left to right: bass-, mid- and treble-control varied individually from 0 dots 1 in steps of 0.1, while the other parameters are set to middle position, value 0.5.*

overlap so that changes in one frequency band will also affect the other bands.

The components in this circuit are: resistors R_0 =38 kΩ and $R_1 = 100\,\text{k}\Omega$, capacitors $C_1 = 250\,\text{pF}$, $C_2 = 100\,\text{nF}$ and $C_3 = 47\,\text{nF}$. The potentiometers $R_2 = 250\,\text{k}\Omega$ and $R_4 = 10\,\text{k}\Omega$ have a linear taper, $R_3 = 250\,\text{k}\Omega$ has logarithmic taper. The load R_L is assumed to be very high so that the load current can be neglected. In this assembly the circuit corresponds to the classic Fender tone stack, type AA763.

3.1. State-Space Model for the Tone Stack

In case of the tone stack schematic, the mesh current analysis is well suited to develop the system equations. We will follow the convention that all voltages and currents are direct from left to right or from top to bottom, respectively.

We consider the first mesh being on the left side including the signal source V_{in}, the internal resistance R_0, continuing with R_1, C_3 and the potentiometer R_4. Kirchhoff's voltage law then postulates

$$-v_{in} + v_{R0} + v_{R1} + v_{C3} + v_{R4} = 0. \tag{20}$$

The voltage v_{R1} can be expressed by the resistor R_1 and the currents through the capacitors C_2 and C_3. For the capacitors the relation

$$i_C = C \cdot \dot{u}_C \tag{21}$$

has to be used (definition of the capacitance), leading to

$$\begin{aligned} v_{R1} &= R_1 \cdot (i_{C2} + i_{C3}) \\ &= R_1 \cdot C_2 \cdot \dot{v}_{C2} + R_1 \cdot C_3 \cdot \dot{v}_{C3}. \end{aligned} \tag{22}$$

For the first mesh we therefore obtain the expression

$$\begin{aligned} -v_{C3} + v_{in} = \; & \dot{v}_{C1} \cdot (R_0 + R_4) \cdot C_1 \\ & + \dot{v}_{C2} \cdot (R_0 + R_1 + R_4) \cdot C_2 \\ & + \dot{v}_{C3} \cdot (R_0 + R_1 + R_4) \cdot C_3. \end{aligned} \tag{23}$$

In the same way the equations for the second and third mesh are found. The complete system can now be described by the matrix formulation

$$\begin{pmatrix} -R_m C_1 & (-R_m - R_1)C_2 & (-R_m - R_1)C_3 \\ -R_2 C_1 & R_1 C_2 & R_1 C_3 \\ R_3 C_1 & R_3 C_2 & 0 \end{pmatrix} \cdot \begin{pmatrix} \dot{v}_{C1} \\ \dot{v}_{C2} \\ \dot{v}_{C3} \end{pmatrix}$$

$$= \begin{pmatrix} 0 & 0 & 1 \\ 1 & -1 & 0 \\ 0 & -1 & 1 \end{pmatrix} \cdot \begin{pmatrix} v_{C1} \\ v_{C2} \\ v_{C3} \end{pmatrix} + \begin{pmatrix} 1 \\ 0 \\ 0 \end{pmatrix} \cdot V_{in} \tag{24}$$

where $R_m = R_0 + R_4$. The output is the tap of potentiometer R_2, controlled by parameter α. For the voltage V_{out} we find the expression

$$V_{out} = V_{in} - V_{R0} - V_{C1} - \alpha V_{R2}. \tag{25}$$

3.2. Discretization

The system description in compliance with equation (1) is achieved by multiplying the inverse of the matrix on the left side of equation (24) to both sides. Expressing the voltages V_{R0} and V_{R2} in equation (25) by the currents through the capacitors and the resistor values leads to an output description in compliance with equation (2). For the tone stack circuit we find the state matrix

$$\boldsymbol{A} = -\frac{1}{R_x} \cdot \tag{26}$$

$$\begin{pmatrix} \frac{R_m+R_1}{C_1} & -\frac{R_m+R_1}{C_1} & \frac{R_1}{C_1} \\ -\frac{R_m+R_1}{C_2} & \frac{R_x+R_3\cdot(R_m+R_1)}{C_2 R_3} & -\frac{R_x+R_1 R_3}{C_2 R_3} \\ \frac{R_1}{C_3} & -\frac{R_x+R_1 R_3}{C_3 R_3} & \frac{R_1 R_2+(R_1+R_2)\cdot(R_m+R_3)}{C_3 R_3} \end{pmatrix}$$

and the input, output and feedthrough vectors

$$\boldsymbol{b} = \begin{pmatrix} \frac{R_1}{C_1 R_x} \\ -\frac{R_1}{C_2 R_x} \\ \frac{R_1+R_2}{C_3 R_x} \end{pmatrix}, \tag{27}$$

$$\boldsymbol{d} = \frac{1}{R_x} \cdot \begin{pmatrix} -R_x + \alpha R_2 \cdot (R_m + R_1) + R_0 R_1 \\ -\alpha R_2 \cdot (R_m + R_1) - R_0 R_1 \\ R_0 R_1 + R_1 \alpha R_2 + R_0 R_2 \end{pmatrix}^T \tag{28}$$

and

$$\boldsymbol{e} = \left(\frac{R_x - R_1 \alpha R_2 - R_0 R_1 - R_0 R_2}{R_x} \right) \tag{29}$$

with $R_x = R_0 R_1 + R_0 R_2 + R_1 R_4 + R_2 R_4 + R_1 R_2$.
The state vector $\boldsymbol{x}$ contains the voltages across the capacitors

$$\boldsymbol{x} = \begin{pmatrix} v_{C1} & v_{C2} & v_{C3} \end{pmatrix}^T \tag{30}$$

and the source is the input voltage $u = V_{in}$.

By utilizing the matrix and vector formulations as given in equation (16) to equation (19), the final discrete-time system is easily derived. When the potentiometer values are varied, the system matrices have to be adapted.

For comparison a system description using the DK-method (see section §2.5) was arranged as well. The equivalent discrete system ends up with a [8 × 8] system matrix, which has to be inverted in case of parameter modifications.

4. STATE-SPACE REPRESENTATION OF NON-LINEAR SYSTEMS

The proposed method from section §2 is now extended to general systems containing non-linear elements, to enable the modeling of circuits containing diodes, transistors or valves.

Let

$$\dot{\boldsymbol{x}} = \boldsymbol{A}\boldsymbol{x} + \boldsymbol{b}u + \boldsymbol{C}\boldsymbol{i}(\boldsymbol{v}) \tag{31}$$

$$y = \boldsymbol{d}\boldsymbol{x} + eu + \boldsymbol{f}\boldsymbol{i}(\boldsymbol{v}) \tag{32}$$

$$\boldsymbol{v} = \boldsymbol{G}\boldsymbol{x} + \boldsymbol{h}u + \boldsymbol{K}\boldsymbol{i}(\boldsymbol{v}) \tag{33}$$

be an extension of the linear system where both the state and the output equation contain a non-linear part $\boldsymbol{i}(\boldsymbol{v})$ that depends on $\boldsymbol{v}$ which is calculated similarly to the output by equation (33). Note that equation (33) is a non-linear equation in $\boldsymbol{v}$. Discretization and canonicalization as in section §2 yields

$$\boldsymbol{x}_c(n) = \bar{\boldsymbol{A}}\boldsymbol{x}_c(n-1) + \bar{\boldsymbol{b}}u(n) + \bar{\boldsymbol{C}}\boldsymbol{i}(\boldsymbol{v}(n)) \tag{34}$$

$$y(n) = \bar{\boldsymbol{d}}\boldsymbol{x}_c(n-1) + \bar{e}u(n) + \bar{\boldsymbol{f}}\boldsymbol{i}(\boldsymbol{v}(n)) \tag{35}$$

$$\boldsymbol{v}(n) = \bar{\boldsymbol{G}}\boldsymbol{x}_c(n-1) + \bar{\boldsymbol{h}}u(n) + \bar{\boldsymbol{K}}\boldsymbol{i}(\boldsymbol{v}(n)) \tag{36}$$

with

$$\bar{\boldsymbol{C}} = 2\left(\tfrac{2}{T}\boldsymbol{I} - \boldsymbol{A}\right)^{-1}\boldsymbol{C} \tag{37}$$

$$\bar{\boldsymbol{f}} = \boldsymbol{f} + \boldsymbol{d}\left(\tfrac{2}{T}\boldsymbol{I} - \boldsymbol{A}\right)^{-1}\boldsymbol{C} \tag{38}$$

$$\bar{\boldsymbol{G}} = \tfrac{2}{T}\boldsymbol{G}\left(\tfrac{2}{T}\boldsymbol{I} - \boldsymbol{A}\right)^{-1} \tag{39}$$

$$\bar{\boldsymbol{h}} = \boldsymbol{h} + \boldsymbol{G}\left(\tfrac{2}{T}\boldsymbol{I} - \boldsymbol{A}\right)^{-1}\boldsymbol{b} \tag{40}$$

$$\bar{\boldsymbol{K}} = \boldsymbol{K} + \boldsymbol{G}\left(\tfrac{2}{T}\boldsymbol{I} - \boldsymbol{A}\right)^{-1}\boldsymbol{C}. \tag{41}$$

4.1. Schedule for non-linear Systems

The computation for a non-linear system proceeds as follows:

1. State-space analysis of the circuit: Find a (symbolic) matrix formulation in the continuous-time domain. The voltages across the capacitors are defining states. Contributions from non-linear elements are expressed by $\boldsymbol{i}(\boldsymbol{v}(n))$.
2. Perform the discretization (e.g. trapezoidal rule) to achieve the discrete-time representation.
3. Filtering process:
   - Solve the non-linear equation given in equation (36) to obtain $\boldsymbol{i}(\boldsymbol{v}(n))$ from the current input $u(n)$ and the previous state $\boldsymbol{x}_c(n-1)$. Here we exploit the fact that equation (36) depends on $\boldsymbol{x}_c(n-1)$, not $\boldsymbol{x}_c(n)$.
   - Once $\boldsymbol{i}(\boldsymbol{v}(n))$ has been determined, the new state and the output are computed with equations (34) and (35).
   - Update the matrix entries in case of parameter changes.

5. APPLICATION: MARSHALL JCM900 PREAMP

The second circuit we want to discuss is part of a Marshall amplifier, namely the "A"-channel of the JCM900 Hi Gain Dual Reverb head, type 4100, see Figure 3. This is a good example for a parametric, non-linear circuit. The distortion is produced by a simple LED network in the feedback path, limiting the amplitude to a maximum of approximately $2\times1.6\,\mathrm{V}$. With the variable resistor R_3 (titled *gain* on the amplifier, parameter α in the simulation) the sound can be controlled from *clean* to *medium drive* and *crunch rhythm* [5]. The resistor values are: R_1 =22 kΩ,

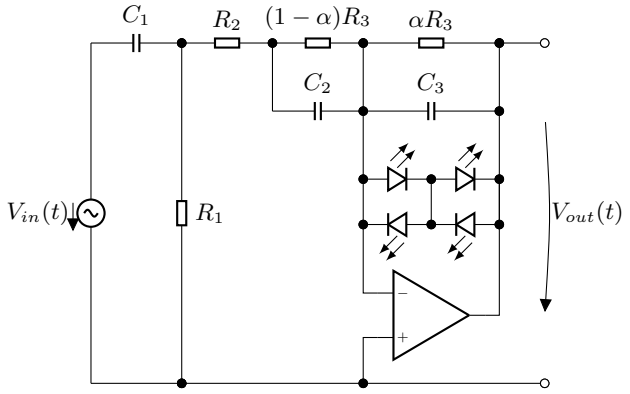

Figure 3: *Schematic of the non-linear part of the JCM900's "A"-channel preamp.*

R_2 =12 kΩ and the potentiometer R_3 =220 kΩ. The gain increases with higher values of α. The capacitors are: C_1 =47 nF, C_2 =1 nF and C_3 =47 pF. The diodes in the original circuit are 3 mm LEDs with red color. The open-loop gain of the used operational amplifier (type M5201) is significantly higher than the maximal gain that can be achieved in this circuit, estimated by $G \approx 20 \cdot \log(\frac{R_3}{R_2}) = 25\,\mathrm{dB}$. In addition, the output amplitude is small compared to the supply voltage. For that reason the operational amplifier is assumed to be ideal for the simulation, i.e. no voltage drop between the inputs.

Modeling the Nonlinear Part

The nonlinearity is given as an antiparallel-series combination of four red LEDs, see the schematic in Figure 3. For the simulation, the LEDs are assumed to be identical such that the voltage drop across one diode is $v_{C_3}/2$. The current i_{D1} through one diode for a given voltage V_F can be calculated by the Shockley-equation

$$i_{D1} = I_s \cdot \left(e^{\frac{V_F}{n \cdot V_t}} - 1\right) \tag{42}$$

with the reverse saturation current I_s = 6.5×10^{-20} A, the thermal voltage V_t = 25.3 mV and the emission coefficient n = 1.68. The capacitance of the pn-junction as well as a series resistance is neglected.

The I-V-transfer function of one LED is shown in Figure 4. For the four-diode combination the non-linear current can be combined and expressed as

$$\begin{aligned}\boldsymbol{i} = i_D &= I_s \cdot (e^{\frac{V_{C3}}{2n \cdot V_t}} - 1) - I_s \cdot (e^{\frac{-V_{C3}}{2n \cdot V_t}} - 1) \\ &= 2I_s \cdot \sinh\left(\tfrac{V_{C3}}{2n \cdot V_t}\right).\end{aligned} \tag{43}$$

Adjustment of the Potentiometer

The potentiometer used in the original amplifier has a S-shaped characteristic. For correct simulation results the control parameter α has to be adjusted. The interpolated function mapping the position of the gain knob to α values, extracted from pointwise measurements, is depicted in Figure 4.

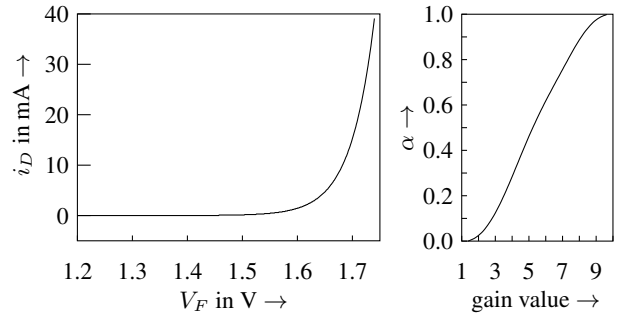

Figure 4: *On the left: I-V transfer function for one red LED. On the right: Mapping gain to α (interpolated).*

5.1. State-Space Model for the JCM900 Preamp

Just like for the tone stack, we start the circuit analysis by expressing the currents through the resistors in terms of the input voltage u and the voltages across the capacitors. This yields the matrix formulation

$$\boldsymbol{A} = \begin{pmatrix} -\frac{R_1+R_2}{C_1R_1R_2} & -\frac{1}{R_2C_1} & 0 \\ -\frac{1}{R_2C_2} & -\frac{R_2+(1-\alpha)R_3}{(1-\alpha)R_2R_3C_2} & 0 \\ -\frac{1}{R_2C_3} & -\frac{1}{R_2C_3} & -\frac{1}{\alpha R_3C_3} \end{pmatrix},$$

$$\boldsymbol{b} = \begin{pmatrix} \frac{R_1+R_2}{C_1R_1R_2} \\ \frac{1}{C_2R_2} \\ \frac{1}{C_3R_2} \end{pmatrix}, \quad \boldsymbol{C} = \begin{pmatrix} 0 \\ 0 \\ -\frac{1}{C_3} \end{pmatrix} \tag{44}$$

in the nomenclature of section §4 with $\boldsymbol{x} = \begin{pmatrix} v_{C_1} & v_{C_2} & v_{C_3} \end{pmatrix}^T$.

The output equation is easily derived, as one terminal of C_3 is at the output node, while the other is at the reference potential (assuming again no voltage drop between the op amp inputs), so that $y = -v_{C_3}$, i.e. $\boldsymbol{d} = \begin{pmatrix} 0 & 0 & -1 \end{pmatrix}$, $e = 0$ and $\boldsymbol{f} = 0$.

Likewise, the current through the diodes is driven by the voltage across C_3, giving $\boldsymbol{G} = \begin{pmatrix} 0 & 0 & 1 \end{pmatrix}$, $\boldsymbol{h} = 0$ and $\boldsymbol{K} = 0$.

5.2. Discretization with efficient handling of parameter α

Again the introduced user-controllable parameter α leads to problems for the discretization. Whenever α changes, the coefficients of the discrete system have to be recomputed. Especially the matrix inversion $(\frac{T}{2}\boldsymbol{I} - \boldsymbol{A})^{-1}$ seems to be quite unattractive.

Fortunately, we can exploit that $\boldsymbol{A}$ has a special structure, namely, it can be rewritten as

$$\boldsymbol{A} = -\begin{pmatrix} C_1 & 0 & 0 \\ 0 & C_2 & 0 \\ 0 & 0 & C_3 \end{pmatrix}^{-1} \left(\begin{pmatrix} \frac{1}{R_1} & 0 & 0 \\ 0 & \frac{1}{(1-\alpha)R_3} & 0 \\ 0 & 0 & \frac{1}{\alpha R_3} \end{pmatrix} + \frac{1}{R_2} \begin{pmatrix} 1 \\ 1 \\ 1 \end{pmatrix} \begin{pmatrix} 1 & 1 & 0 \end{pmatrix} \right). \tag{45}$$

The matrix inversion can then be rewritten as

$$(\tfrac{2}{T}\boldsymbol{I} - \boldsymbol{A})^{-1} = \left(\begin{pmatrix} \beta_1^{-1} & 0 & 0 \\ 0 & \beta_2^{-1} & 0 \\ 0 & 0 & \beta_3^{-1} \end{pmatrix} + \frac{1}{R_2} \begin{pmatrix} 1 \\ 1 \\ 1 \end{pmatrix} \begin{pmatrix} 1 & 1 & 0 \end{pmatrix} \right)^{-1} \cdot \begin{pmatrix} C_1 & 0 & 0 \\ 0 & C_2 & 0 \\ 0 & 0 & C_3 \end{pmatrix} \tag{46}$$

with

$$\beta_1 = \frac{R_1T}{2C_1R_1 + T}, \qquad \beta_2 = \frac{(1-\alpha)R_3T}{2(1-\alpha)C_2R_3 + T} \text{ and}$$
$$\beta_3 = \frac{\alpha R_3T}{2\alpha C_3R_3 + T}. \tag{47}$$

The inversion now lends itself to applying the Sherman-Morrison formula, finally giving

$$(\tfrac{T}{2}\boldsymbol{I} - \boldsymbol{A})^{-1} = \left(\boldsymbol{I} - \frac{1}{R_2 + \beta_1 + \beta_2} \begin{pmatrix} \beta_1 \\ \beta_2 \\ \beta_3 \end{pmatrix} \begin{pmatrix} 1 & 1 & 0 \end{pmatrix} \right) \cdot \begin{pmatrix} \beta_1C_1 & 0 & 0 \\ 0 & \beta_2C_2 & 0 \\ 0 & 0 & \beta_3C_3 \end{pmatrix}. \tag{48}$$

This allows to derive the following relatively simple formulas for the coefficients:

$$\bar{\boldsymbol{A}} = \begin{pmatrix} \frac{2C_1R_1-T}{2C_1R_1+T} & 0 & 0 \\ 0 & \frac{2(1-\alpha)C_2R_3-T}{2(1-\alpha)C_2R_3+T} & 0 \\ 0 & 0 & \frac{2\alpha C_3R_3-T}{2\alpha C_3R_3+T} \end{pmatrix} - \frac{4}{R_1T \cdot (R_2 + \beta_1 + \beta_2)} \begin{pmatrix} \beta_1 \\ \beta_2 \\ \beta_3 \end{pmatrix} \begin{pmatrix} \beta_1C_1 & \beta_2C_2 & 0 \end{pmatrix}$$

$$\bar{\boldsymbol{b}} = -\frac{2}{R_1 \cdot (R_2 + \beta_1 + \beta_2)} \begin{pmatrix} \beta_1 \cdot (R_1 + R_2 + \beta_2) \\ \beta_2 \cdot (R_1 - \beta_1) \\ \beta_3 \cdot (R_1 - \beta_1) \end{pmatrix}$$

$$\bar{\boldsymbol{C}} = -2 \begin{pmatrix} 0 \\ 0 \\ \beta_3 \end{pmatrix}$$

$$\bar{\boldsymbol{d}} = \tfrac{2}{T} \cdot \begin{pmatrix} \beta_1C_1 \cdot \frac{\beta_3}{R_2+\beta_1+\beta_2} & \beta_2C_2 \cdot \frac{\beta_3}{R_2+\beta_1+\beta_2} & -\beta_3C_3 \end{pmatrix}$$

$$\bar{e} = -\frac{\beta_3(R_1 - \beta_1)}{(R_2 + \beta_1 + \beta_2)R_1}$$

$$\bar{\boldsymbol{f}} = \beta_3$$

$$\bar{\boldsymbol{G}} = -\bar{\boldsymbol{d}}$$

$$\bar{\boldsymbol{h}} = -\bar{e}$$

$$\bar{\boldsymbol{K}} = -\beta_3$$

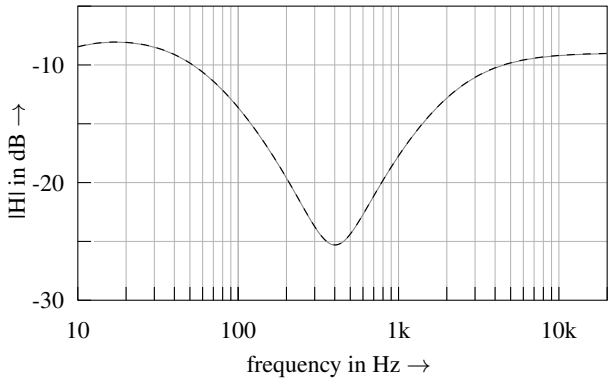

Figure 5: *Frequency response comparison: LT Spice simulation as reference (gray) and state-space model (dashed black) of the tone stack circuit. Bass-, mid- and treble-control were set to 0.5.*

Again the DK-method is applied to the same system to estimate the computational costs for the recalculation of coefficients. The equivalent discrete system has the dimension [7×7]. Using the formulation as above the dimensions are reduced and the numerical inversion can be avoided. The circumvention of the matrix inversion can of course not be generalized to other circuits, but the methodology will be similar.

6. RESULTS

To evaluate how true to original the simulations perform, the output data has been compared to measurements or other reliable references.

6.1. Tone Stack Simulation

The tone stack is a simple linear system, therefore it is uncomplicated to find reference data. The frequency responses calculated with the simulation are compared to responses from the software tool *The Tone Stack Calculator* [6] and a simulation using LT Spice IV and show good match, as shown in Figure 5.

6.2. JCM900 Preamp Simulation

For the preamp circuit from section §5 the original Marshall top is used as reference. Thus the evaluation becomes more complicated concerning various aspects: First of all, the signal amplitudes used in simulation and measurements have to fit very well. Then one has to ensure that all component values and all parameters are equal. Third, the measurements are done inside the noisy environment of the amplifier. Deviations can be explained by component tolerances in the measured system and simplifications (e.g. ideal OPA) in the simulation. All measurements and simulations are performed with a sampling frequency $f_s = \frac{1}{T} = 96\,\text{kHz}$.

Waveforms

A qualified test signal is given by single frequency sine bursts with an exponentially decaying envelope, which imitate the transient shape of real guitar signals. Burst signals with various levels and frequencies are used at different gain settings. The test set contains all 63 possible combinations of

- amplitude at the input jack: $200\,\text{mV}$, $500\,\text{mV}$ and $1\,\text{V}$,
- burst frequency: $500\,\text{Hz}$, $1\,\text{kHz}$ and $2\,\text{kHz}$ and
- potentiometer *gain*-values $4 \ldots 10$ (max), adjusted on the Marshall amplifier.

The test signal is fed into the input jack of the amplifier and than recorded simultaneously before and after the wanted preamp stage. The signal recorded at the input of the preamp stage now can be applied to the input of the simulation, allowing a direct comparison with the measurement.

The dependency of the output waveform for different input levels is displayed in Figure 6. All measurements and simulations are performed with the same gain settings and frequency. Figure 7 shows the waveforms for different gain values. As the plots illustrate, a high similarity is achieved.

Harmonic Spectra

Besides the evaluation of the waveforms, the harmonic content of the output is computed both for reference system and simulation. By using a variant of the exponential sweep technique, introduced by Farina [7], the *harmonic impulse responses* (HIR) can be measured [8]. The related harmonic transfer functions give explicit information about the harmonic distortion and can be considered as a form of fingerprint describing the static part of the nonlinearity as mentioned in [9].

Figures 8(a) and 8(b) show the harmonic spectra when the *gain*-knob is turned to 6 of 10. The fundamental frequency response (in black) as well as the strong odd components (in dashed gray) are in good accordance. For the minor even harmonic components there is no observable similarity.

In Figures 8(c) and 8(d) both reference and simulation are adjusted to maximum gain, 10 of 10. The fundamental frequency response, all odd components as well as second and forth harmonic (k2, k4) have a close match. Again there is no visible similarity for the higher order even harmonics. Please note: Because the stimulating signal was fed to the input jack, the (linear) influence of the pre-located input stage is also captured in these plots. It is noticeable that the even components depart from the measurements. One possible explanation is the fact that the LEDs in the original circuit are not exactly equal, so that the nonlinearity is slightly asymmetric and not ideally symmetric.

Guitar Music

In addition some sound clips of electric guitar playing are recorded. The clips are available on our homepage

`http://ant.hsu-hh.de/dafx10`

Please note that a guitar signal recorded at this point, without the influence of the subsequent amplifier stages and the loudspeaker, will not sound very pleasant. On that account all sound clips were afterwards processed with a loudspeaker simulation of a typical guitar cabinet for enhancement. The comparison supports the good conformance of the results.

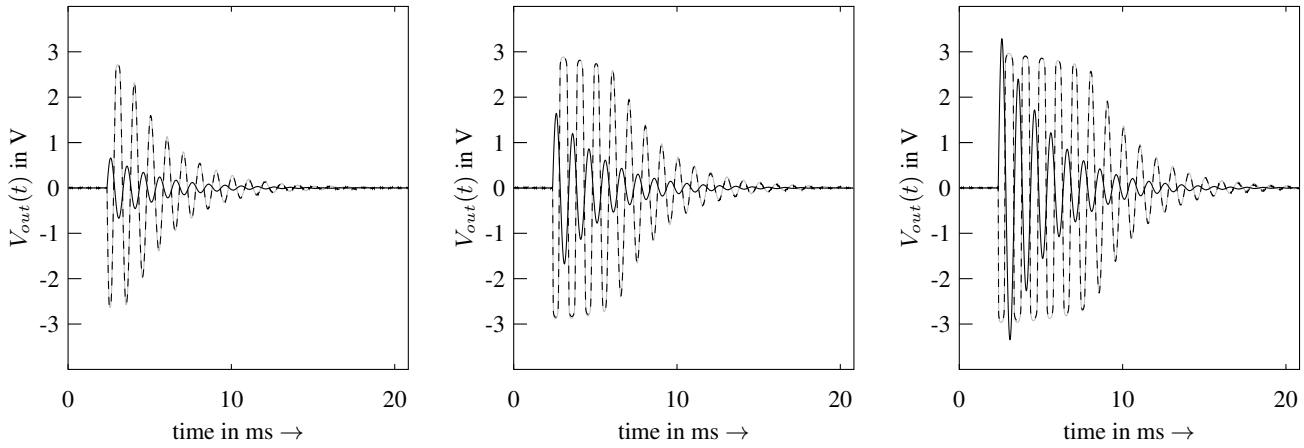

Figure 6: *Waveform comparison of measurement (gray) and simulation (dashed black). Stimulation with sine burst (solid black) with frequency* 1 kHz *for gain 8 of 10. From left to right: input level* 200 mV*,* 500 mV *and* 1 V.

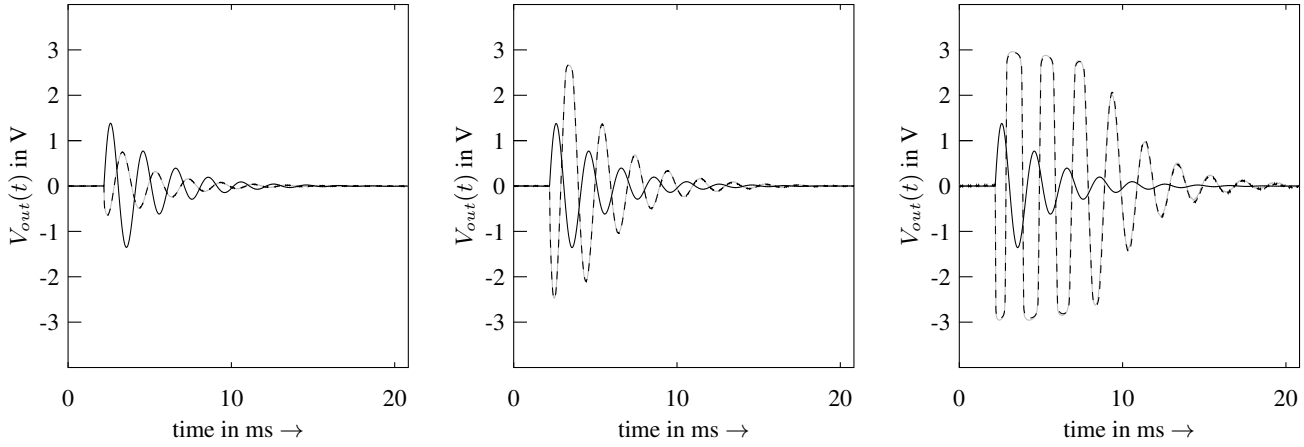

Figure 7: *Waveform comparison of measurement (gray) and simulation (dashed black). Stimulation with sine burst (solid black) with frequency* 500 Hz *and input level* 500 mV. *On the left: gain value 4 of 10, mid: 7 of 10 and on the right: 10 of 10.*

7. CONCLUSIONS

A state-space representation for the digital simulation of analog audio circuits was presented and extended to a canonical and minimized formulation. Descriptions for linear and non-linear systems were given and derived step-by-step. It was pointed out that parametric components like potentiometers may lead to either high computational costs or high memory requirements. With the linear passive filter network *tone stack* and the non-linear distorting preamp two parametric subcircuits found in typical guitar amplifiers were analyzed as examples.

Solutions for the simulation of both systems using state-space representations and trapezoidal rule discretization were presented and explained. To evaluate how true to original the simulations perform, the output data was compared to reference data, mainly in terms of measurements from the accordant original circuit. For the distorted preamp, the waveforms of the output signals processed by the simulation and measured in the reference system were in good accordance for different test signals. The harmonic spectra showed a good match, too. Some short music samples of an electric guitar bring the comparison to completion.

It was shown that the computational costs in case of recalculation of the coefficients are reduced compared to the related DK-method, due to the minimized matrix formulations. Thus this method is applicable for real-time simulation. A drawback is that the network analysis is more complicated and has to be done manually. Nevertheless the presented method is well applicable for the simulation of parametric circuits and provides good results.

8. REFERENCES

[1] J. Pakarinen, M. Tikander, and M. Karjalainen, "Wave digital modeling of the output chain of a vacuum-tube amplifier," in *Proc. of the 12th Int. Conf. on Digital Audio Effects (DAFx-09)*, Como, Italy, Sept. 1–4 2009, pp. 55–59.

[2] D.T. Yeh, *Digital Implementation of Musical Distortion Cir-*

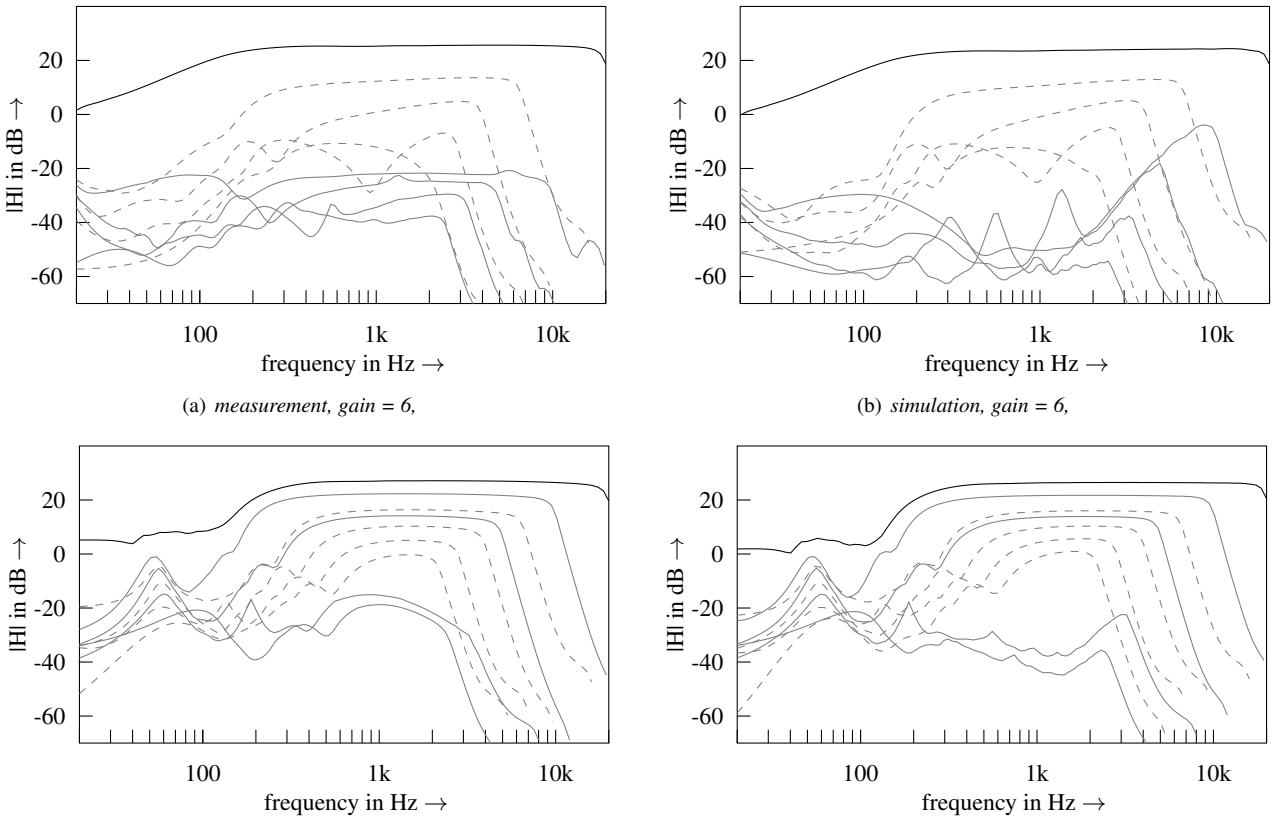

(a) *measurement, gain = 6,*

(b) *simulation, gain = 6,*

(c) *measurement, gain = 10 and*

(d) *simulation, gain = 10.*

Figure 8: *Smoothed harmonic spectra of the reference system on the left side and of the simulations on the right. Fundamental (black), odd (dashed gray) and even order harmonic responses (solid gray).*

cuits by Analysis and Simulation, Ph.D. dissertation, Stanford University, June 2009.

[3] J. Pakarinen and D. Yeh, "A review of digital techniques for modeling vacuum-tube guitar amplifiers," *Computer Music Journal*, vol. 33, no. 2, pp. 85–100, 2009.

[4] D.T. Yeh and J.O. Smith, "Discretization of the '59 Fender bassman tone stack," in *Proc. of the 9th Int. Conf. on Digital Audio Effects (DAFx-06)*, Montreal, Quebec, Canada, Sept. 18–20 2006, pp. 1–6.

[5] Marshall Amplification plc, Milton Keynes, England, *Marshall JCM900 Handbook*, Nov. 1998.

[6] Duncan Amplification, "Tone stack calculator, version 1.3.0.36," [Online] http://www.duncanamps.com/tsc, Retrieved February 20th 2010.

[7] A. Farina, "Simultaneous measurement of impulse response and distortion with a swept-sine technique," in *108th AES Convention*, Paris, France, Feb. 19-24 2000.

[8] S. Müller, "Measuring transfer-functions and impulse responses," in *Signal Processing in Acoustics*. 2008, vol. 1, pp. 74–76, D. Havelock, S. Kuwano and M. Vorländer (Eds.), Springer.

[9] K. Dempwolf, M. Holters, S. Möller, and U. Zölzer, "The influence of small variations in a simplified guitar amplifier model," in *Proc. of the 12th Int. Conf. on Digital Audio Effects (DAFx-09)*, Como, Italy, Sept. 1–4 2009, pp. 127–132.